Crack width evaluation in post-tensioned prestressed concrete bridge-deck slabs

Y.C. Choi & B.H. Oh
Dept. of Civil Engineering, Seoul National University, Seoul, Korea

S.L. Lee
Dept. of Civil Engineering, Mokpo National University, Muan-gun, Jeonnam, Korea

S.W. Yoo
Dept. of Civil Engineering, Woosuk University, Wanju-gun, Jeonbuk, Korea

M.K. Lee
Dept. of Civil Engineering, Jeonju University, Jeonju-si, Jeonbuk, Korea

B. S. Jang
Dam Engineering Research Center, Korea Water Resources Corporation, Daejeon, Korea

ABSTRACT: The purpose of the present study is to investigate the cracking behavior and crack width of transversely post-tensioned concrete decks in PSC box-girder bridges. For this purpose, full-scale box-girder members were made and tested. Major test variables include the amount of prestressing and prestressing steel ratios. The crack width, strains and deflections of deck slabs were measured automatically according to the increase of applied loads. The bond effectiveness of prestressing steel was determined from the test data and it was found to be about 0.468 compared with non-prestressed ordinary rebar. A realistic formula for predicting crack width of PSC deck slabs has been derived. The comparison of proposed equation agrees very well with test data while the existing Gergely-Lutz equation and CEB-FIP code equation show large deviation from the test data. The proposed equation can be efficiently used for the realistic analysis and design of prestressed concrete decks in box-girder bridges

1 INTRODUCTION

The transverse prestressing of bridge decks was first introduced in box-girder bridges mainly to maximize the length of cantilever overhangs and to reduce the number of webs (Almustafa 1983, Oh et al. 2005). The post-tensioning system is generally used in the transverse prestressing of bridge decks in box-girder bridges (Figure 1). Recently, it was reported that many serious longitudinal cracks occurred at the bottom of top slab of prestressed concrete (PSC) box-girder bridges which are not prestressed laterally (Almustafa 1983, Oh et al. 2005). The transverse prestressing reduces definitely the widths of longitudinal cracks. The crack widths must be limited to certain allowable values especially in PSC structures under service loads. It is therefore necessary to have a realistic prediction equation for crack width under applied loading for rational and safe design of PSC box-girder bridges.

In the post-tensioned prestressed members, prestressing steel stresses are transferred from the prestressing steel via the surrounding grout to the duct, containing the prestressing tendon, and from the duct to the structural concrete (Almustafa 1983). It is generally difficult to evaluate the local bond behavior of prestressing tendon because the tendons are partly in contact with the duct and partly with the surrounding concrete. It is therefore necessary to identify the effective circumference of multi-strands in which the strands are bonded to concrete. The purpose of the present study is first to investigate the bond behavior of prestressing steel and then to propose a realistic formula for predicting maximum crack width of PSC deck slabs. The maximum crack width is derived in terms of steel stress which represents the magnitude of applied loadings. For this purpose, four full-scale box girder members were fabricated and tested. The major objective of the present tests was to see the transverse behavior of PSC box-girders including the cracking behavior of upper deck slabs.

Many strain gages were installed on transverse rebars and prestressing steels to measure the strain changes under applied loads. The crack width gages were also installed to monitor the variation of crack widths at the bottom surface of top slab during the loading process. From the comparisons of the strains of PS steels with the strains of nonprestressed rebars at the same locations, the bond characteristic of post-tensioned steel was evaluated. The proposed equation for maximum crack width is a function of steel stress after decompression, effective tensile area, bond characteristic parameter of PS steel, and diameter of steel bar. To verify the applicability of proposed equation, the proposed formula is compared with test data, Gergely and Lutz equation (1968) and CEB-FIP model code (1990).

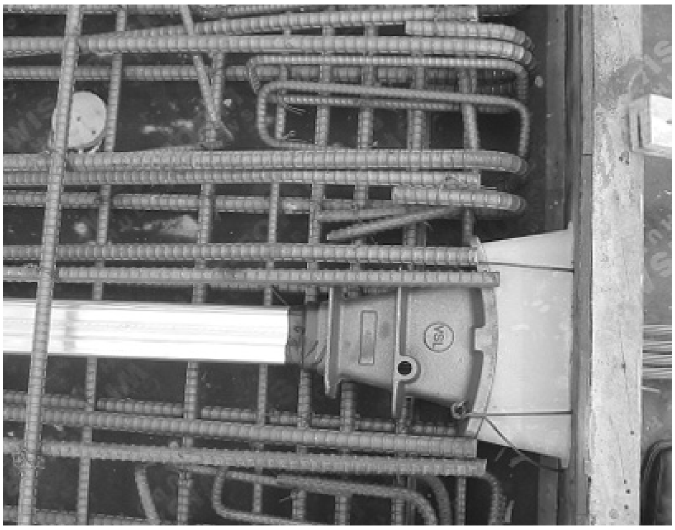

Figure 1. Transverse post-tensioning system of bridge deck in box girder bridges.

2 BOND MECHANISM OF PRESTRESSED CONCRETE MEMBERS

The cracking of prestressed concrete members is influenced by the interaction between steel and concrete. Between adjacent cracks the tensile forces are transferred form the steel to the surrounding concrete by bond stress. The distribution of the bond stress along the bar is generally nonlinear. Since the distance between the cracks varies, it is difficult to calculate the exact distributions of bond stresses between steel and concrete. In order to simplify the calculation, the analysis is based on an average constant bond stress (CEB-FIP 1990, Alvarez & Marti 1996) along the bar and it is also assumed that the tensile strength of the concrete does not vary over the length of the bar. Alvarez & Marti (1996) analyzed the cracked prestressed concrete tension members with the approximate distributions of bond stresses for the reinforcing bar and prestressing steel. The basic equilibrium in tension requires that the total tensile force is equal to the sum of the tensile forces of the reinforcing bar and prestressing steel.

The CEB-FIP model code (1990) considers that the bond behavior of prestressing tendons is different form that of deformed reinforcing bars. The different magnitude of steel stress develops in prestressing steel and reinforcing bar, respectively. The CEB-FIP code (1990) considers two stages separately for crack formation, i.e., single crack formation phase and stabilized crack formation phase. For single crack formation phase, the different transmission lengths l_s and l_p for bond stresses are calculated for reinforcing bar and prestressing steel, respectively, with the assumption of equal crack widths for prestressing and reinforcing steels. The increase of stress after cracking is much less in prestressing steel than in reinforcing steel. For stabilized multiple cracking phase, the transmission length is considered to be equal for prestressing steel and reinforcing bar, which is calculated by considering the different diameters and different bond behavior of reinforcing bars and prestressing steels, respectively. However, the effect of multiple strands in a duct on the bond behavior of prestressing steel was not considered in these calculations in the code (CEB-FIP model code 1990). As can be seen in the next section of present paper, however, the effects of multi-strands in a duct must be considered correctly in order to obtain realistic bond behavior and thus reasonable crack width equation for prestressed concrete members

3 EXPERIMENTAL INVESTIGATION

3.1 *Outline of Test Members*

Four full-scale concrete box girder members have been designed and made to investigate the crack width and crack spacing of deck slab in PSC box-girder bridges. The transverse width, longitudinal length and total height of test members of concrete box girders are 6,500mm, 2,300mm and 1,600mm, respectively as shown in Figure 2. The main design variables include the magnitude of precompression, diameter of steel bars, non-prestressed steel ratio and prestressing steel ratio in the top slab of box-girder bridges. Figure 2 shows the detailed section A-A′ of top slab of test members. The magnitudes of precompression due to lateral prestressing are 0, 2.35, 3.52, and 4.70 MPa for test member LP0, LP1, LP2, and LP3, respectively. This is to see the effect of prestressing on the control of crack width under service loads.

3.2 *Material Properties*

The regular deformed bars have been used in the present test members. The yield strength of mild reinforcement was 398MPa from material tests in the laboratory. The steel strain gages were installed at the transverse reinforcements. Those gages were protected by covering them with proper waterproof materials. In this study, all prestressing steels were uncoated, low-relaxation 15.2mm seven-wire strands and the flat duct (70×20mm) were used to locate the tendons inside. The yield and ultimate strength of the strands were 1,600MPa and 1,892MPa, respectively. To evaluate the strain increase of tendon after cracking, the steel strain gages were also installed with adequate protection. The concrete was carefully placed in the form so as not to hurt the attached steel strain gages and the maximum-size of aggregate was 25mm (1in.). The concrete cylinders with size of ø100×200mm were cast and cured under similar curing condition of test members. The average compressive strength concrete was 40MPa.

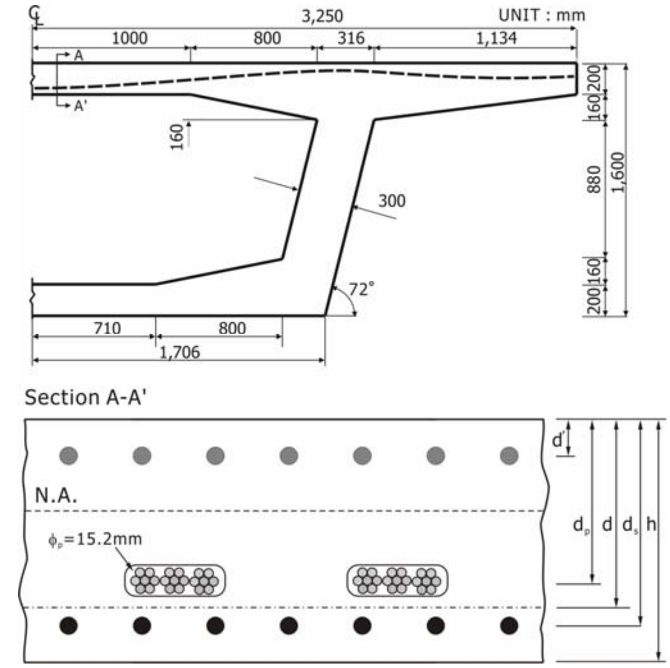

Figure 2. Schematic diagram for cross section properties.

3.3 *Measurement*

Transverse post-tensioning was conducted by using the mono-hydraulic jack. The jacking stress of prestressing steel was $0.75f_{pu}$. The test members were loaded at two points on the upper deck, which simulate two lateral wheel loads. The concrete surfaces were painted white with emulsion paint to facilitate the measurement of crack propagation. The load was applied to the test members using the automatically controlled actuators. The linear variable differential transducers (LVDTs) were installed to measure the deflection profiles of the top slab of the box-girder.

In order to monitor the flexural crack width under applied load, the crack width gages were attached over the cracks after reading the initial values of crack width with microscopes. All strain values of ordinary bars and prestressing tendons and the crack width values at concrete surface were automatically measured and stored in the computer during the loading process. The number of cracks and crack spacings were also measured at each loading step.

4 TEST RESULTS AND ANALTYSIS

4.1 *Bond Characteristics of Post-Tensioned Steel*

When prestressed steels and ordinary rebars are simultaneously used, different amounts of steel stresses are expected to develop in prestressed steel and ordinary rebar because the bond behavior of prestressing tendons is different from that of reinforcing bars.

Figure 3 shows the relationship between the increases of tendon stress and rebar stress after decompression for test member LP1. It can be seen that fairly good linear relations are obtained between the increments of tendon stress and ordinary rebar stresses. The increment of tendon stress is about 46.8 percent (0.468) on the average of that of ordinary rebar stress. This indicates that the effectiveness of bond property of prestressing steels is much lower than that of ordinary ribbed bars. The bond effectiveness ratio may be set as about 0.468 between prestressing steel and ordinary rebar from the present test results.

For single crack formation stage in a prestressed member, the relationship between the bond stresses of prestressing steel and ordinary rebar may be written as follows according to CEB-FIP model code (1990).

$$\Delta f_p = \sqrt{\frac{\tau_{ap}\sum_{op} A_s}{\tau_{as}\sum_{os} A_p}} f_s = \sqrt{\frac{\tau_{ap}\phi_s}{\tau_{as}\phi_p}} f_s \quad (1)$$

where Δf_p, f_s= increments of tendon and reinforcing bar stresses after decompression, ϕ_p, ϕ_s = nominal diameters of strand and reinforcing bar, τ_{ap}, τ_{as} = average bond stresses of tendon and rebar, respectively, $\sum_{op}$, $\sum_{os}$ = effective circumferential perimeter of multi-strands in a flat duct and reinforcing bar, and A_p, A_s = total area of multiple strands in a flat duct and the area of reinforcing bar, respectively.

Equation 1 neglects the effect of multi-strands in a duct. In flat duct systems, the tendons are partly in contact with the duct and partly with concrete. In order to identify the bond property between concrete and tendon, it is necessary to determine the circumferential perimeter of multi-strands which are directly bonded to surrounding grout materials. In this study, the effective circumferential perimeter of multi-strands is derived as Equation 2.

$$\sum_{op} = \pi\phi_p + (n-1)\phi_p \quad (2)$$

Where n is the number of strand in a flat duct.

Equation 1 is now then modified by using the effective circumference of multiple strands in a duct.

$$\Delta f_p = \sqrt{\frac{\tau_{ap}}{\tau_{as}}\frac{\sum_{op}}{A_p}\frac{\phi_s}{4}} f_s = \sqrt{\frac{\tau_{ap}}{\tau_{as}}\frac{\pi+(n-1)}{n\pi}\frac{\phi_s}{\phi_p}} f_s = \xi f_s \quad (3)$$

The relation between Δf_p and f_s of Equation 3 can be obtained from the test data of Figure 3. The average value of these ratios between Δf_p and f_s was obtained as 0.468. Now, the value of τ_{ap}/τ_{as} can be obtained from Equation 3 with the test results of Figure 3. The average value of τ_{ap}/τ_{as} was found to be 0.465 from the present test data. The CEB-FIP code (1990) specifies the value of τ_{ap}/τ_{as} to be 0.4 for post-tensioned strands, which is somewhat lower than the average value from the present test results. The present test data indicate that CEB-FIP model code (1990) overestimates the circumferential perimeter for multiple strands within a duct.

4.2 *Crack Occurrence*

The transverse flexural cracks were firstly appeared in the top slab at an approximately applied load of 500kN for all test members. The first longitudinal flexural cracks of top slabs were formed at the applied load of 550kN, 564kN, 643kN and 916kN (where 1kN=220.46lb) for LP0, LP1, LP2 and LP3, respectively. This indicates that test member LP3 which has largest precompressive stress exhibits much higher initial cracking load. This can be seen clearly from the present test results which show less cracking at the same applied load levels as the precompression increases.

In pure bending region, the crack spacing was investigated for various increasing load levels. The average crack spacing decreases with increase of load level which means that the number of cracks increases as the applied load increases. The increase of prestressing force (LP3) exhibits rather large crack spacing. The average crack spacing may be a function of prestressing steel ratio.

4.3 *Derivation of Crack Width Formula*

The phenomenon of cracking of concrete is complex because of the tensile weakness of concrete. The crack width may depend on many factors such as steel stress, effective concrete area in tension, nonprestressed reinforcement type and ratio, prestressing steel type and ratio, and strength of concrete.

If time-dependent effects are considered in the PSC members, the stress of ordinary rebar will increase due to creep deformation of concrete.

In this study, the increase of ordinary steel stress due to time-dependent effects after prestressing has been taken care of and only the increment of steel stress after decompression has been considered to compare with crack width increase according to load increase.

The relationship between rebar stress after decompression and maximum crack width can be assumed to be linear (Bazant & Oh 1983, Gergely & Lutz 1968, Oh & Kang 1997). The value of crack width is also generally assumed to increase in proportion to the diameter of rebar (Oh & Kang 1997). The effective concrete area in tension accounts for the non-uniform normal stress distribution arising from bond forces into the concrete cross-section at the end of the transmission length.

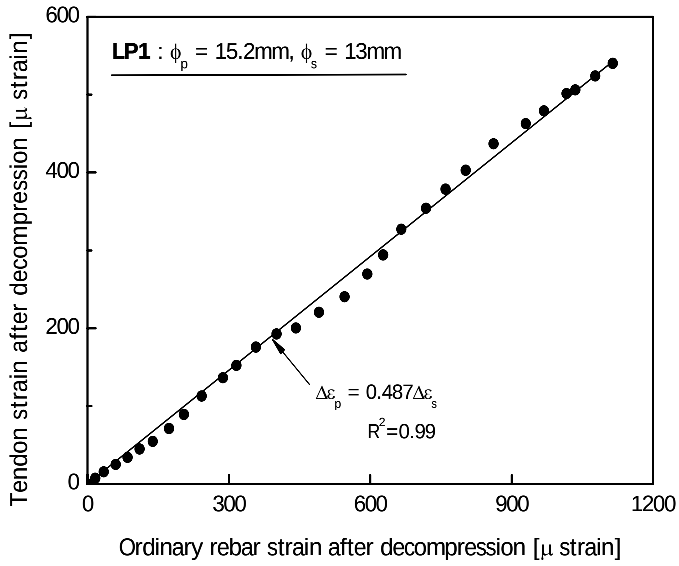

Figure 3. Relationship between tendon and reinforcing bar strains after decompression for LP1 test members.

In this study, the effective concrete area in tension is written as Equation 4 which is given by CEB-FIP model code (1990).

$$A_{t,eff} = \min[2.5(c + \phi_s/2)b, (h-x)b/3] \tag{4}$$

where c is concrete clear cover depth, x is the neutral axis depth of fully cracked section and b is the width of member.

Figure 4 shows the nonlinear relationship between the ratio $w_{max}/f_s\phi_s$ and the ratio ρ_{eff} [= $(A_{st}+\xi A_{pt})/A_{t,eff}$] which are obtained from the test results. The value of ξ represents the bond effectiveness between the prestressing steel and ordinary rebar. The value of ρ_{eff} [= $(A_{st}+\xi A_{pt})/A_{t,eff}$] may be defined as the effective combined reinforcement ratio of ordinary rebar plus effective prestressing steel with reference to effective tensile concrete area.

Figure 4 shows that the crack width decreases with an increase of effective combined reinforcement ratio ρ_{eff} and is inversely proportional to $\rho_{eff}^{0.75}$. From this relation of ρ_{eff} with crack width w_{max}, the maximum crack width equation is reasonably derived as follows.

$$w_{max} = 3\times10^{-6}(f_s - f_0)\phi_s\left(\frac{A_{t,eff}}{A_{st}+\xi A_{pt}}\right)^{0.75}\frac{h-x}{d-x} \tag{5}$$

$$\xi = \sqrt{\frac{\tau_{ap}}{\tau_{as}}\frac{\pi+(n-1)}{n\pi}\frac{\phi_s}{\phi_p}} \tag{6}$$

where w_{max} = predicted maximum crack width in mm, A_{st}, A_{pt} = total area of prestressing steels and reinforcing bars, x = neutral axis depth of cracked section in mm, h = height of cross section in mm, d = effective depth in mm, ϕ_s = diameter of rebar in mm, ϕ_p = diameter of PS strand in mm, f_s = increment of rebar stress after decompression in MPa, f_0 = steel stress at the initial occurrence of crack in MPa, and τ_{ap}/τ_{as} is 0.465 for post-tensioned tendons which was obtained from this study. Here, *(h-x/d-x)* was introduced to represent the crack width at the bottom face of flexural members.

Generally, the cracking starts at the tensile strain of about 0.0002 in concrete. Therefore, the reinforcement stress after decompression at the first occurrence of crack is 40MPa (5800psi) because the cracking strain of concrete is about 0.0002. Therefore, the realistic prediction equation of crack width is now reasonably suggested as follows.

$$w_{max} = 3\times10^{-6}\left(f_s - 40\right)\phi_s\left(\frac{A_{t,eff}}{A_{st}+\xi A_{pt}}\right)^{0.75}\frac{h-x}{d-x} \qquad (7)$$

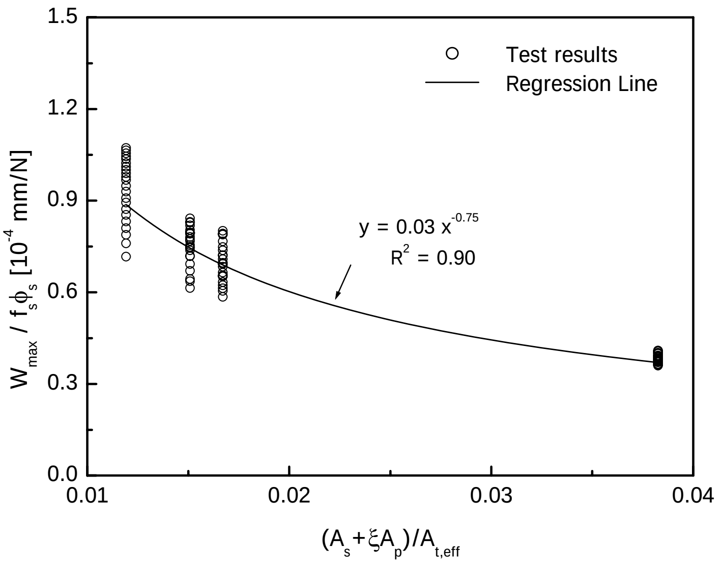

Figure 4. Correlation between effective reinforcement ratio and observed crack width.

5 COMPARISON WITH TEST DATA

The proposed crack width formula has been compared with the present test results. Figure 5 shows the comparisons of proposed crack width equation with the experimental data. Figure 5 also shows the comparisons with the simplified crack width equation of Gergely and Lutz (1968) and maximum crack width equation of CEB-FIP Model Code (1990) which consists of two parts, i.e., single crack formation phase and stabilized crack formation phase.

Gergely and Lutz equation overestimates the observed maximum crack widths for all test members. This is probably due to the fact that Gergely and Lutz equation is basically based on the test data of reinforced concrete members. On the other hand, the CEB-FIP model code equation generally underestimates the maximum crack width especially in the lower stress range of reinforcing bar. This may be due to the fact that the CEB-FIP code (1990) considers two different stages in the crack formation separately, i.e., single crack formation phase and stabilized crack formation phase.

However, it can be clearly seen from the test data of Figure 5 that the crack width increases almost linearly form the initial stage. The proposed equation agrees very well with test data for all stress ranges. Therefore, the suggested formula may well be used for the realistic analysis and design of deck slabs in prestressed concrete box-girder bridges.

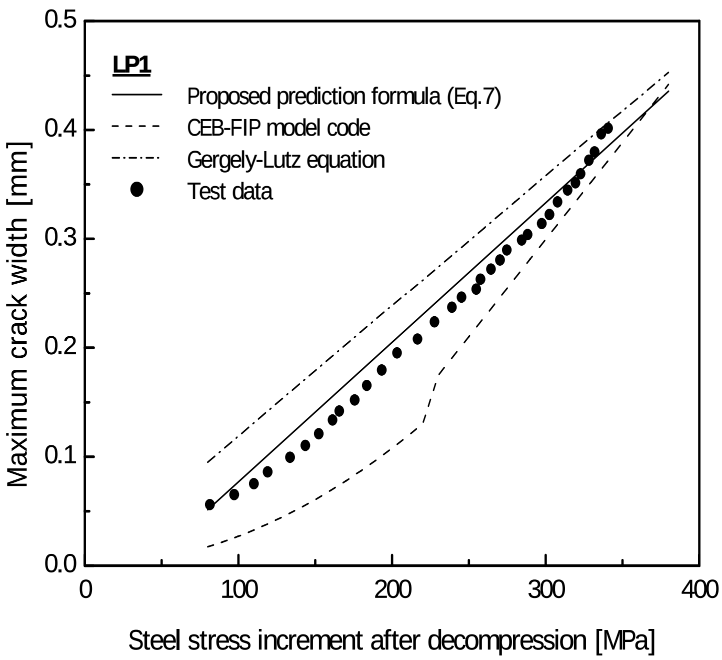

Figure 5. Comparison of proposed crack width equation with experimental data.

6 CONCLUSION

The purpose of the present study is to explore the cracking behavior of laterally prestressed bridge decks in box-girder bridges. For this purpose, a series of full-scale box girders have been fabricated and tested.

The bond characteristics of prestressing steels were identified from the measurements of strains for both prestressing steels and ordinary rebars. The bond effectiveness of prestressing steels was obtained from the present test results and it was found to be about 0.468 compared with ordinary rebars.

The effective circumferential perimeter of multi-strands in a duct which is bonded to concrete is derived and used to determine the crack width under applied loads. A realistic prediction equation for crack widths was derived in terms of effective combined reinforcement ratio, diameter of rebar, and the rebar stress after decompression.

The proposed equation correlates very well with test data of crack width under applied loads, while the existing formulae of CEB-FIP and Gergely & Lutz equation deviate greatly from the test data for prestressed concrete flexural members.

REFERENCES

Almustafa, R.A. 1983. *The analysis of transverse prestressing effects in bridge decks*: 6-7. PH.D. thesis. The university of Texas at Austin.

Bažant, Z.P. & Oh, B.H. 1983. Spacing of cracks in reinforced concrete. *Journal of Structural Engineering, ASCE* 109(9): 2066-2085.

Alvarez, M. & Marti, P. 1996. Experimental bond behavior of reinforcing steels at plastic strains. *Institut für Baustatik, ETH*, Zurich, Switzerland: 134.

Comite-Euro International du Beton/Federation Internationale de la Precomtrainte. *CEB-FIP Model Code 1990*: 274-255. London: Thomas Telford.

Gergely, P. & Lutz, L.A. 1968. Maximum crack width in reinforced concrete flexural members. *Causes, Mechanism, and Control of Cracking in Concrete*. SP-20: 87-117. Detroit: American Concrete Institute

Oh, B.H et al. 2005. Flexural behavior of PSC box girders according to haunch size. *Journal of KSCE*, 25(2-A): 217-280.

Oh, B.H. & Kang, Y.J. 1997. New formulas for maximum crack width and crack spacing in reinforced concrete flexural members. *ACI Journal*, March-April: 103-112.